Kinetic approach to a relativistic Bose-Einstein condensate

Alex Meistrenko,[1,*] Hendrik van Hees,[1,2,†] Kai Zhou,[1,2,‡] and Carsten Greiner[1,§]

[1] *Institut für theoretische Physik, Goethe-Universität Frankfurt am Main, Max-von-Laue-Straße 1, 60438 Frankfurt, Germany*

[2] *Frankfurt Institute for Advanced Studies, Ruth-Moufang-Straße 1, 60438 Frankfurt, Germany*

(Dated: February 18, 2016)

We apply a Boltzmann approach to the kinetic regime of a relativistic Bose-Einstein condensate of scalar bosons by decomposing the one-particle distribution function in a condensate part and a non-zero momentum part of excited modes, leading to a coupled set of evolution equations which are then solved efficiently with an adaptive higher order Runge-Kutta scheme. We compare our results to the partonic cascade Monte-Carlo simulation BAMPS for a critical but far from equilibrium case of massless bosons. Motivated by the color glass condensate initial conditions in QCD with a strongly overpopulated initial glasma state, we also discuss the time evolution starting from an overpopulated initial distribution function of massive scalar bosons. In this system a self-similar evolution of the particle cascade with a non-relativistic turbulent scaling in the infrared sector is observed as well as a relativistic exponent for the direct energy cascade, confirming a weak wave turbulence in the ultraviolet region.

I. INTRODUCTION

An ultracold atomic gas is a well-known and celebrated example of a Bose-Einstein condensate (BEC) that arises close to the absolute zero point of the temperature T [1]:

$$f(E_i) = \frac{1}{\exp\left(\frac{E_i-\mu}{T}\right)-1} \xrightarrow[T\to 0]{} 0 \quad \text{for} \quad E_i > E_0 \geq \mu\,. \tag{1}$$

Thus in case of the Bose statistics the occupation number of all energy states E_i above the ground state E_0 becomes arbitrarily small. Consequently, all particles of the system occupy the ground state, leading to a macroscopic ground-state occupation number and forming a coherent as well as a strongly correlated state. In astrophysics it was proposed that dark matter, which is assumed to be a cold bosonic and gravitationally bound system, could exist in the form of a BEC [2]. For compact stars the condensation of mesons [3] is discussed or even Cooper pairing of baryons, which then can undergo a crossover transition to a BEC state [4]. Many more examples can be found in condensed-matter theory, like condensation of magnons, which are quasiparticles of spin waves. Magnons can condensate far from the absolute zero point, to be more precise at room temperature [5]. Hence, there are two different possibilities for the formation of a BEC state either by decreasing the temperature or by increasing the particle density of bosons until it exceeds a critical value. In this case the chemical potential becomes equal to the energy of the ground state

$$f(E_0) = \frac{1}{\exp\left(\frac{E_0-\mu}{T}\right)-1} \xrightarrow[\mu\to E_0]{} \infty \quad \text{for} \quad E_0 = m \geq \mu\,, \tag{2}$$

leading once more to a macroscopic occupation number of E_0. However, in the thermodynamic limit of 3 spatial dimensions with $\mathrm{d}^3p \sim p^2\mathrm{d}p$ one does not obtain a macroscopic particle number for $\mu \to m$ in the soft region by integrating the momentum distribution function $f = \mathrm{d}N/\mathrm{d}^3x\mathrm{d}^3p$ as seen from the expansion $E = \sqrt{m^2+p^2} \simeq m + p^2/2m$. Thus one has to treat the BEC in the kinetic regime as an extra contribution $\sim \delta^{(3)}(\vec{p})$ to the one-particle distribution function as will be discussed in Sec. II.

Since our motivation originates from high-energy physics, where we study the chiral phase transition in the linear σ model [6–9], we focus in Sec. III on initially overpopulated conditions similar to the initial state of a heavy-ion collision. Due to ultrarelativistic energies the two incoming heavy ions can be considered as two slices of color glass condensate (CGC) which form a strongly overpopulated initial glasma state during the collision process [10]. This state is highly dominated by gluons and could lead on a short time scale to the formation of a condensate-like state for gluons when in the kinetic regime binary scatterings dominate over chemical processes [11–16]. Such a condensate state would be highly relativistic, since the relevant saturation scale Q_s is of the order of 1 GeV, corresponding to the square root of the initial number of partons per unit transverse area. Thereby the occupation number is proportional to the inverse QCD coupling constant $\alpha_s(Q_s) \ll 1$ up to the saturation scale

$$f(t=0,p) \sim \frac{1}{\alpha_s} \quad \text{for} \quad p < Q_s\,, \tag{3}$$

which suggests a perturbative treatment of the QCD in

* meistrenko@th.physik.uni-frankfurt.de
† hees@fias.uni-frankfurt.de
‡ zhou@th.physik.uni-frankfurt.de
§ Carsten.Greiner@th.physik.uni-frankfurt.de

this limit.

In Sec. II we derive a set of evolution equations from the general form of the Boltzmann equation and describe briefly our numerical strategy for solving directly the partial integro-differential equations. We then compare our results in Sec. III to the partonic cascade simulation BAMPS (Boltzmann Approach to Multi-Parton Scatterings) [17, 18], which applies a stochastic test particle ansatz to solve the collision integrals. Finally, we discuss the dynamical evolution, starting from a strongly overpopulated initial condition.

II. BOLTZMANN APPROACH WITH CONDENSATION

We start with the general expression for the time-dependent relativistic Boltzmann-Uehling-Uhlenbeck equation

$$\begin{aligned}\partial_t f\left(t,\vec{p}_1\right) =& \frac{1}{2E_1}\int\frac{\mathrm{d}^3\vec{p}_2}{\left(2\pi\right)^3 2E_2}\int\frac{\mathrm{d}^3\vec{p}_3}{\left(2\pi\right)^3 2E_3}\int\frac{\mathrm{d}^3\vec{p}_4}{\left(2\pi\right)^3 2E_4}\\ &\times\left(2\pi\right)^4\delta^{(4)}\left(P_1+P_2-P_3-P_4\right)\frac{\left|\mathcal{M}_{12\to34}\right|^2}{\nu}\\ &\times\left[\left(1+f_1\right)\left(1+f_2\right)f_3 f_4\right.\\ &\left.\quad -f_1 f_2\left(1+f_3\right)\left(1+f_4\right)\right],\end{aligned} \tag{4}$$

where $f_i := f\left(t,\vec{p}_i\right)$ with $i\in\{1,2,3,4\}$ denotes the one-particle distribution function, ν is the degeneracy factor, and P_i stands for the particle's on-shell four-momentum, $P_i^0 = E_{\vec{p}_i} = \sqrt{m_i^2+\vec{p}_i^2}$. Following similar lines as in reference [19] we decompose the distribution function in two parts,

$$\begin{aligned}f\left(t,\vec{p}\right) &= f_{\mathrm{part}}\left(t,\vec{p}\right)+f_{\mathrm{cond}}\left(t,\vec{p}=0\right)\\ &= f_{\mathrm{part}}\left(t,\vec{p}\right)+n_{\mathrm{cond}}\left(t\right)\left(2\pi\right)^3\delta^{(3)}(\vec{p})\,.\end{aligned} \tag{5}$$

The first expression $f_{\mathrm{part}}\left(t,\vec{p}\right)$ denotes the distribution function of non-zero momentum modes (particles), whereas the second one $f_{\mathrm{cond}}\left(t,\vec{p}=0\right)$ contains the condensate contribution at zero momentum. The latter part is proportional to the condensate density $n_{\mathrm{cond}}\left(t\right)$ and a δ-function in momentum space. By inserting the decomposition (5) in (4) and comparing the coefficients, one derives the evolution equation for the condensate,

$$\partial_t f_{\mathrm{cond}}\left(t,\vec{p}_1=0\right) = \mathcal{C}_{1\mathrm{c}+1\mathrm{p}\leftrightarrow 2\mathrm{p}}\,, \tag{6}$$

with the condensate-particle collision term

$$\begin{aligned}\mathcal{C}_{1\mathrm{c}+1\mathrm{p}\leftrightarrow 2\mathrm{p}} =& \frac{1}{2E_1}\int\frac{\mathrm{d}^3\vec{p}_2}{\left(2\pi\right)^3 2E_2}\int\frac{\mathrm{d}^3\vec{p}_3}{\left(2\pi\right)^3 2E_3}\int\frac{\mathrm{d}^3\vec{p}_4}{\left(2\pi\right)^3 2E_4}\\ &\times\left(2\pi\right)^4\delta^{(4)}\left(P_1+P_2-P_3-P_4\right)\frac{\left|\mathcal{M}_{12\to34}\right|^2}{\nu}\\ &\times\left[f_{\mathrm{c}} f_3 f_4 - f_{\mathrm{c}} f_2\left(1+f_3+f_4\right)\right].\end{aligned} \tag{7}$$

The evolution equation for the non-zero modes of the distribution function consists of two collision integrals,

$$\partial_t f_{\mathrm{part}}\left(t,\vec{p}_1\neq 0\right) = \mathcal{C}_{2\mathrm{p}\leftrightarrow 2\mathrm{p}}+\mathcal{C}_{1\mathrm{p}+1\mathrm{c}\leftrightarrow 2\mathrm{p}}\,, \tag{8}$$

which include the pure particle as well as the particle-condensate interactions,

$$\begin{aligned}\mathcal{C}_{1\mathrm{p}+1\mathrm{c}\leftrightarrow 2\mathrm{p}} =& \frac{1}{2E_1}\int\frac{\mathrm{d}^3\vec{p}_2}{\left(2\pi\right)^3 2E_2}\int\frac{\mathrm{d}^3\vec{p}_3}{\left(2\pi\right)^3 2E_3}\int\frac{\mathrm{d}^3\vec{p}_4}{\left(2\pi\right)^3 2E_4}\\ &\times\left(2\pi\right)^4\delta^{(4)}\left(P_1+P_2-P_3-P_4\right)\frac{\left|\mathcal{M}_{12\to34}\right|^2}{\nu}\\ &\times\Big\{\left[f_{\mathrm{c}} f_3 f_4 - f_{\mathrm{c}} f_1\left(1+f_3+f_4\right)\right]\\ &\quad+\left[\left(1+f_1+f_2\right)f_{\mathrm{c}} f_4 - f_{\mathrm{c}} f_1 f_2\right]\\ &\quad+\left[\left(1+f_1+f_2\right)f_{\mathrm{c}} f_3 - f_{\mathrm{c}} f_1 f_2\right]\Big\}.\end{aligned} \tag{9}$$

Due to energy-momentum conservation the condensate part appears only once per gain and loss term of expressions (7) and (9). The collision integral $\mathcal{C}_{2\mathrm{p}\leftrightarrow 2\mathrm{p}}$ has the same structure as the right-hand side of (4), including only non-zero modes.

The evolution of the condensate is fully described by the condensate density since the δ-function can be integrated out

$$\begin{aligned}\partial_t n_{\mathrm{cond}}\left(t\right) &= \int\frac{\mathrm{d}^3\vec{p}_1}{\left(2\pi\right)^3}\partial_t f_{\mathrm{cond}}\left(t,\vec{p}_1=0\right)\\ &= \int\frac{\mathrm{d}^3\vec{p}_1}{\left(2\pi\right)^3}\mathcal{C}_{1\mathrm{c}+1\mathrm{p}\leftrightarrow 2\mathrm{p}}\\ &= -\int\frac{\mathrm{d}^3\vec{p}_1}{\left(2\pi\right)^3}\mathcal{C}_{1\mathrm{p}+1\mathrm{c}\leftrightarrow 2\mathrm{p}}\,.\end{aligned} \tag{10}$$

Because of the last relation the total particle density is conserved, and particles with zero momentum can be interpreted as constituent parts of the condensate.

For a first study of BEC dynamics we focus on an isotropic system of scalar bosons with ϕ^4-interaction[1]

$$\frac{1}{\nu}|\mathcal{M}_{12\to34}|^2 = 18\lambda^2\,. \tag{11}$$

In this case the evolution equations (6) as well as (8) simplify and have the form given by (A10), (A11).

The growth of the condensate happens exponentially fast as can be seen from the form of (A11). This requires an efficient numerical solution of the integro-differential equations. Therefore we use an adaptive numerical scheme and apply the following steps.

[1] We choose $\mathcal{L}_{\mathrm{int}} = \frac{\lambda}{4}\phi^4$ as the quartic interaction term in the Lagrangian.

1. We introduce a non-uniform discretization for the external p_1-momentum with decreasing resolution from the soft to the hard region of momenta, such that the distribution function is now given on a large grid $G := \{p^0, p^1, ..., p^N\}$ with $N > 100$. Thereby for the soft discrete momenta the relation $0 < p^1 < ... < p^k < m$ with $k \gg 1$ holds. That fulfills a mandatory condition in the infrared, reproducing the right scaling close to equilibrium as shown later in Eq. (17).

2. We note that according to the form of (A11) the onset of the condensation process can only happen for a finite initial value of $n_{\mathrm{c}}(t=0)$. It was shown in [20] that the time evolution is independent of the initial value as long as $n_{\mathrm{c}}(t=0)$ is negligibly small compared to the total particle density n_{tot} of the system. Since the condensate starts to grow rapidly when the effective chemical potential[2] of the system becomes equal to the boson mass, it is also possible to insert an initial seed for n_{c} at this time point. Both methods result in almost equal time scales for the condensation process.

   We solve the isotropic two-dimensional collision integrals in (A10) and (A11) for every external mode by applying quadrature methods. The single integrals for the external momentum modes are independent of each other and we can solve them in parallel. Due to the fact that p_4 is integrated out with the energy δ-function, in general it does not lie exactly on the grid. For this momentum the distribution function is interpolated by using cubic splines on the discrete values of the grid G.

   When needed also Monte Carlo importance sampling [21] can be used to calculate the collision integrals. In this case the distribution function is interpolated for all internal momenta p_2, p_3 and p_4.

3. Finally, the differential equations themselves are solved with the Cash-Karp RK45-scheme [22] that guarantees an adaptive slowing down of the simulation during the condensation process and a fast convergence due to the 5^{th}-order accuracy with respect to the time discretization Δt of the scheme.

A different implementation of a discrete Boltzmann equation for scalar particles in (2+1) dimensions and overpopulated systems can be found in [23]. Here, the authors applied their code to a longitudinally expanding system with CGC-like initial conditions, which mimics the kinematics of a heavy ion collision at very high energies.

[2] Obtained from a fit to the Bose distribution function (15).

III. THERMALIZATION IN OVERPOPULATED SYSTEMS

As discussed in Sec. I Bose-Einstein condensation can arise in ultracold or overpopulated systems. Motivated by the color-glass initial conditions in ultrarelativistic heavy-ion collisions, we focus on an isotropic step function as initial momentum distribution and consider the case of overpopulation for scalar bosons

$$f(t=0,p) = f_0\,\theta\left(1-\frac{p}{Q_s}\right). \tag{12}$$

Here $Q_s = 1$ GeV denotes the saturation scale, and $f_0 \sim \mathcal{O}(1)$ is a constant[3]. The total particle as well as energy densities are then given by

$$\begin{aligned} n_{\mathrm{tot}} &= \frac{f_0 Q_s^3}{6\pi^2}\,, \\ \epsilon_{\mathrm{tot}} &= \frac{f_0}{16\pi^2}\Bigg[Q_s E_{Q_s}\left(m^2+2Q_s^2\right) \\ &\qquad + m^4 \log\frac{m}{Q_s+E_{Q_s}}\Bigg] \end{aligned} \tag{13}$$

with m being the mass of the bosons and $E_{Q_s} = \sqrt{m^2+Q_s^2}$. Starting with a nonequilibrium initial condition the system has to end up in an equilibrium distribution function, to be more precise in a Bose distribution. However, in an overpopulated and particle conserving system it will be in general not possible to fit the total particle and energy density at the same time. Consequently, such a system requires that a macroscopic number of particles populates the ground state, i.e., the formation of a Bose-Einstein condensate becomes necessary to reach an equilibrium state. The time evolution of the condensate density is directly related to the evolution of the one-particle distribution function by the following relations:

$$\begin{aligned} n_{\mathrm{cond}}(t) &= n_{\mathrm{tot}} - n_{\mathrm{part}}(t)\,, \\ n_{\mathrm{part}}(t) &= \int \frac{\mathrm{d}^3\vec{p}}{(2\pi)^3} f_{\mathrm{part}}(t,\vec{p})\,, \\ \epsilon_{\mathrm{cond}}(t) &= \epsilon_{\mathrm{tot}} - \epsilon_{\mathrm{part}}(t)\,, \\ \epsilon_{\mathrm{part}}(t) &= \int \frac{\mathrm{d}^3\vec{p}}{(2\pi)^3} E f_{\mathrm{part}}(t,\vec{p})\,. \end{aligned} \tag{14}$$

At thermal equilibrium this set of equations can be solved self-consistently, leading to the Bose distribution as the equilibrium distribution function of non-zero modes:

$$\begin{aligned} f_{\mathrm{B}}(E) &= \frac{1}{\exp\left(\frac{E-\mu}{T}\right)-1} \\ \text{with} \quad E &= \sqrt{p^2+m^2}\,. \end{aligned} \tag{15}$$

[3] Typically, in the gluon saturation regime one obtains $f_0 \approx 2-4$.

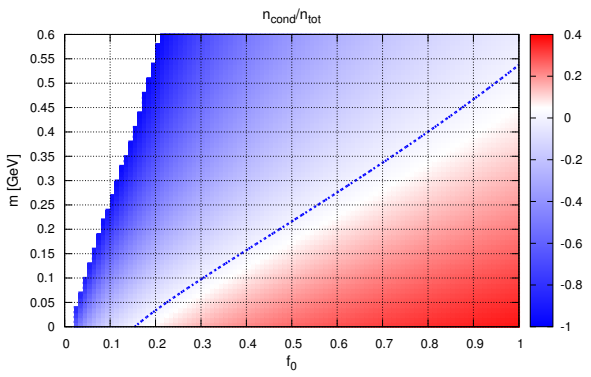

FIG. 1. Numerical solution of (14) for the condensate fraction $n_{\rm cond}/n_{\rm tot}$ under the assumption of $\mu = m$ as a function of the mass m and the step height f_0. Below the blue line a Bose-Einstein condensate forms. The region above the blue line is unphysical since the condition $\mu = m$ does not apply anymore.

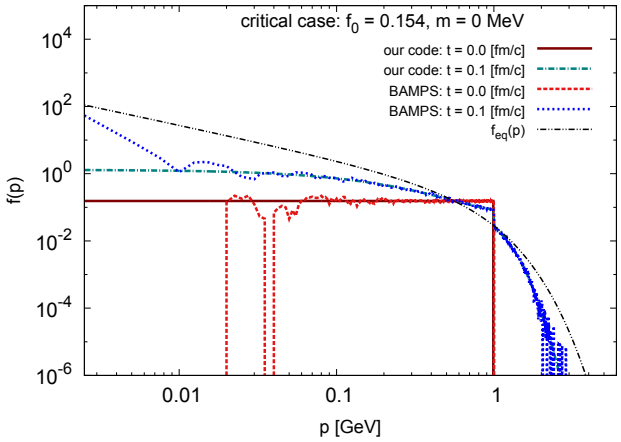

FIG. 2. Momentum distribution function at $t = 0.1$ fm/c, starting from a step function with $f_0 = 0.154$, $m = 0$ MeV. For comparison also BAMPS results (from a single run) of massless bosons are plotted.

In case of BEC formation the chemical potential in (15) becomes $\mu = m$. So the only unknowns are the critical temperature $T_{\rm crit}$ and the condensate density $n_{\rm cond}$, since the energy density is given by the relation $\epsilon_{\rm cond} = m\, n_{\rm cond}$. Fig. 1 shows the numerical solution of (14) for the condensate fraction $n_{\rm cond}/n_{\rm tot}$ in equilibrium as a function of the mass m and the step height f_0. A condensate formation occurs below the blue line, which marks the critical case of $n_{\rm part} = n_{\rm tot}$. The unphysical region of negative values for $n_{\rm cond}$ above the blue line results from the assumption $\mu = m$, which was applied to solve (14).

A. Dynamics of the critical case

Before considering strongly overpopulated systems for massive scalar bosons, we compare the dynamical evolution of the critical case with the well-established partonic transport code BAMPS, which has been developed for gluon and quark transport in heavy-ion collisions. It employs a test-particle ansatz to approximate the phase-space distribution and then solves the collision integrals via a stochastic interpretation [17, 18]. We note that BAMPS treats gluons as massless bosons, and therefore close to equilibrium the momentum distribution function shows the following scaling in the infrared regime (15):

$$f\,(p) \sim \frac{T}{p} \quad \text{for} \quad p \ll T\,, \tag{16}$$

whereas in the massive case one obtains

$$f\,(p) \sim \frac{2mT}{p^2} \quad \text{for} \quad p \ll m \ll T\,. \tag{17}$$

Thus in the very soft region the momentum distribution function of massless bosons behave differently in compar-

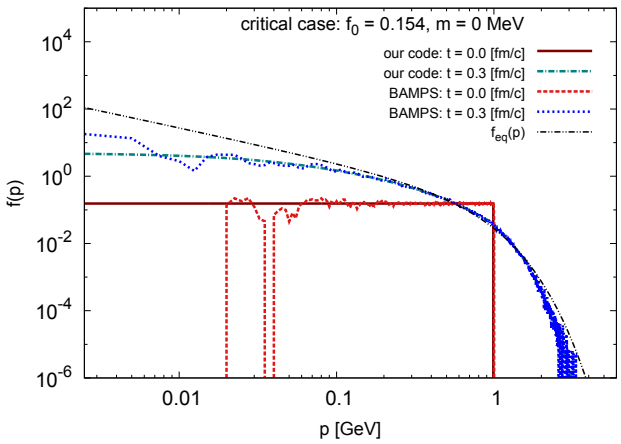

FIG. 3. The same as Fig. 2 but for $t = 0.3$ fm/c

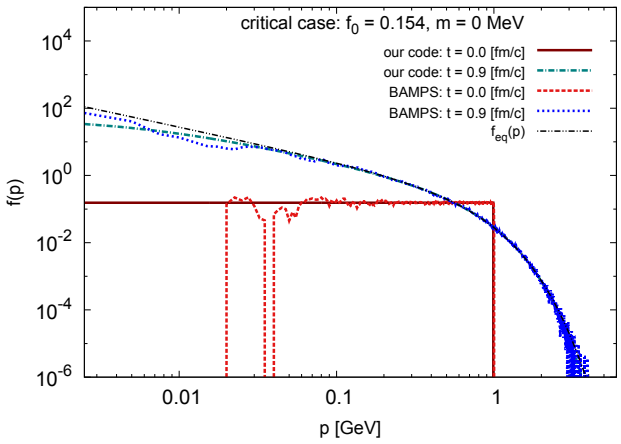

FIG. 4. The same as Fig. 2 but for $t = 0.9$ fm/c with the system being close to the equilibrium state.

ison to massive bosons.

For the numerical comparison we initialize a single BAMPS run with a cross section equivalent to the transition amplitude of the ϕ^4-theory (11) with a relatively large coupling constant $\lambda \approx 46.4$ which reproduces the typical thermalization scale of QCD. According to Eqs. (A10), (A11) a massless approach like BAMPS is applicable for a vanishing value of the condensate[4]. Also in our simulation we can handle the massless case, noting that now the numerical condition in the soft region of discrete momenta has to fulfill $0 < p^1 < ... < p^k < T$ with $k \gg 1$ for being able to reproduce the correct infrared behavior as seen from the form of (16).

Figs. 2-4 show the evolution of the momentum distribution functions for both simulations at three intermediate times between the initial and final states. In the critical case of massless bosons the initial step height is $f_0 = 0.154$ as can be seen from Fig. 1. The dynamics of our simulation is in good agreement with the BAMPS calculation. Only in the soft region the evolution differs due to a lack of statistics in a single run of BAMPS.

B. Dynamics of the strongly overpopulated state

We initialize a strongly overpopulated system according to (12) with $f_0 = 1$, $Q_s = 1$ GeV and a boson mass of $m = 100$ MeV. Since the thermalization scale is simply proportional to $1/\lambda^2$ all results are plotted independently of the coupling constant with $\lambda^2 t$ on the abscissa. Fig. 5 shows the time evolution for the effective temperature and chemical potential as well as the fugacity defined as $z := \exp(\mu/T)$. The onset of condensation happens at around $\lambda^2 t \approx 40$ fm/c when the chemical potential in the soft region shortly overshoots the equilibrium value of $\mu_{\rm eq} = 100$ MeV and then converges rapidly to $\mu_{\rm eq}$. Also the effective temperature converges exactly to the expected value of $T_c \approx 410.57$ MeV leading to $z \approx 1.28$. In addition Figs. 6 and 7 show the evolution of different ratios for the quantities $n_{\rm cond}$, $n_{\rm part}$ as well as $\epsilon_{\rm cond}$, $\epsilon_{\rm part}$. These plots underline the conservation of the total densities $n_{\rm tot}$, $\epsilon_{\rm tot}$ to high accuracy.

Now, we consider the time evolution of the one-particle distribution function. Starting from such a strongly overpopulated state the distribution function grows by 5 orders of magnitude for $p =$ 2-3 MeV and overshoots significantly the equilibrium distribution function. The reason is a strong particle cascade to the infrared, resulting in an inverse energy flow to the ultraviolet region as will be discussed in the following. Due to the onset of the condensation process around $\lambda^2 t \approx 40$ fm/c the particle number of the soft momenta starts to decrease and converges rapidly to the equilibrium shape, whereas the hard

[4] Consequently, a finite value of the condensate requires massive bosons for the simple transition amplitude of the ϕ^4-theory (11).

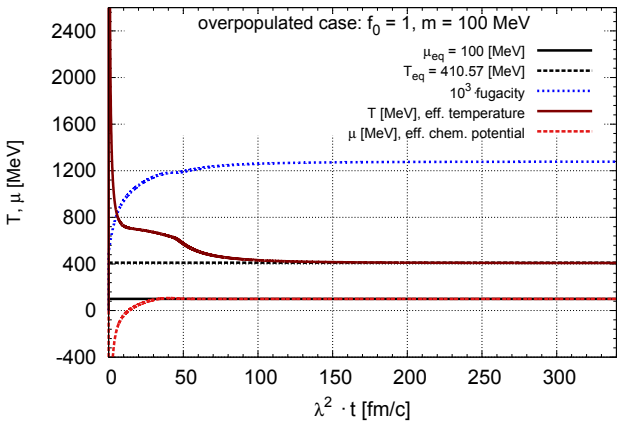

FIG. 5. Evolution of the effective temperature T, chemical potential μ and fugacity as a function of $\lambda^2 t$ for $f_0 = 1$, $m =$ 100 MeV.

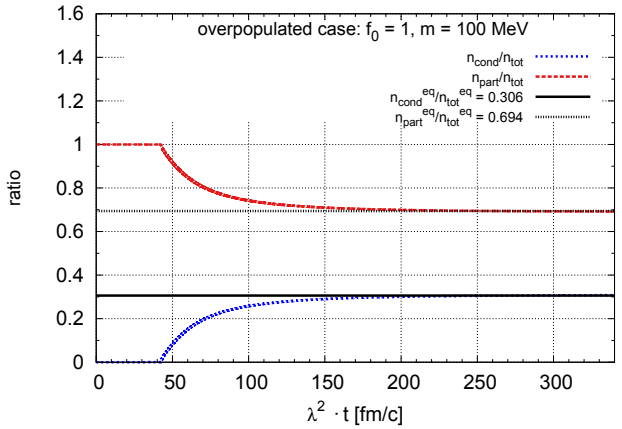

FIG. 6. Evolution of the condensate density $n_{\rm cond}$ with respect to the total particle density $n_{\rm tot}$ as a function of $\lambda^2 t$ for $f_0 = 1$, $m = 100$ MeV.

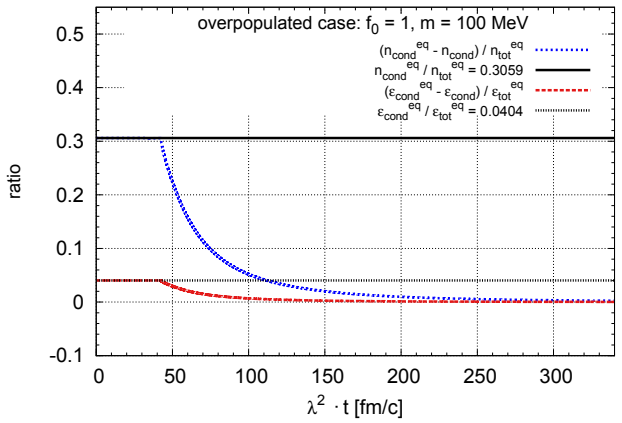

FIG. 7. Relative deviation from equilibrium values of the condensate density $n_{\rm cond}$ and energy density $\epsilon_{\rm cond}$ as a function of $\lambda^2 t$ for $f_0 = 1$, $m = 100$ MeV.

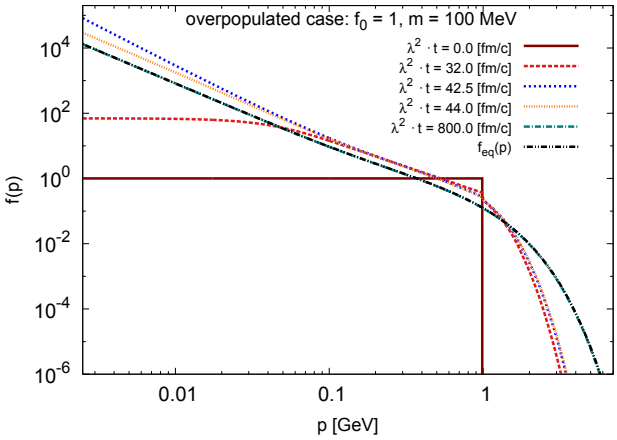

FIG. 8. Time evolution of the one-particle momentum distribution function, starting from an overpopulated initial state, with respect to the coupling-independent time scale $\lambda^2 t$ for $f_0 = 1$ and $m = 100$ MeV.

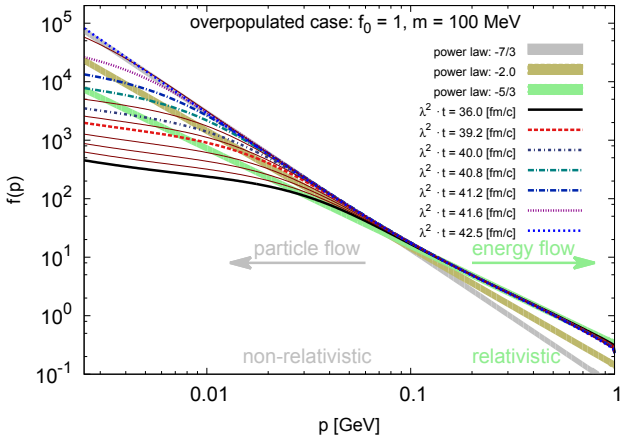

FIG. 9. Self-similar evolution with different power-law scalings of the one-particle distribution function in the region of relativistic and non-relativistic momenta, thin lines indicate intermediate propagation.

modes develop slowly in time, resulting in a large equilibration time compared to the time scale of the condensation. As already seen in Fig. 5 for the effective temperature and chemical potential, the evolution of the system reaches the equilibrium state as a stable fixed point. In the equilibrium state a finite value of the condensate coexists with a Bose distribution function at non-zero momenta. Thereby the condensate value matches exactly the expected value of $n_{\mathrm{cond}} = 0.673\ \mathrm{fm}^{-3}$ which once more underlines the accurate convergence of our kinetic approach (compare also Fig. 10 and 11).

To discuss the one-particle distribution function in detail we focus on references [19, 24], where the authors studied the evolution of a similar system in a classical approach with the dispersion relation $E = p^2/2m$ and analyzed the energy scaling in detail. Thereby they observed a self-similar evolution in time before the onset of the condensation process and obtained a particular power law $f(E) \sim 1/E^{\alpha}$ with the numerical exponent $\alpha_{\mathrm{num}} \approx 1.24$ in the deep infrared region, which was close to the value $\alpha = 7/6$. It was pointed out by the authors that the exponent α marks a non-thermal fixed point for the distribution function and acts as a root for the collision integral of the classical Boltzmann equation as can be shown by means of a Zakharov transformation[5]. Consequently, there exists an energy scale, where the occupation number changes only slowly in time. Due to particle and energy conservation a self-similar evolution of this energy scale can be observed, growing in time and propagating towards the infrared. To be more precise they found a turbulent transport of scalar bosons to the infrared, which is known as an inverse particle cascade.

Fig. 9 summarizes the evolution (resolved in time) for the overpopulated system with the initial state $f_0 = 1$, starting from $\lambda^2 t = 36\ \mathrm{fm}/c$ up to the time at which the one-particle distribution function reaches its maximum. Obviously, one observes two regions with almost linear scalings in a double logarithmic plot. We denote the momentum range with $p \ll m$ as non-relativistic, whereas $p \gg m$ marks the relativistic regime. In fact, both exponents can be understood from examination of the scaling behavior of the collision integral. Therefore, we consider the individual terms of the Boltzmann equation (4) in App. B under momentum rescaling.

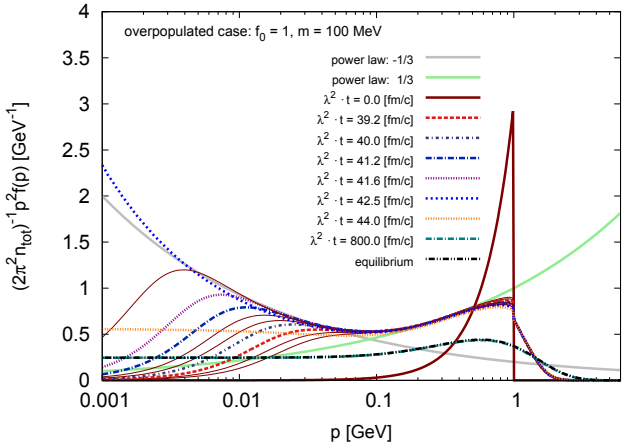

FIG. 10. Differential fraction of the isotropic particle density with respect to the momentum, showing different power-law scalings in the region of relativistic and non-relativistic momenta.

To obtain a feeling for particle and energy transport, we also plotted the differential particle as well as energy density in Figs. 10 and 11 for an isotropic system with

[5] Further references can be found in [24].

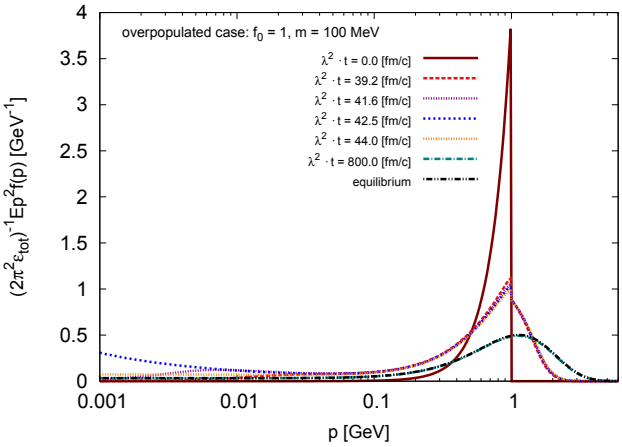

FIG. 11. Differential fraction of the isotropic energy density with respect to the momentum.

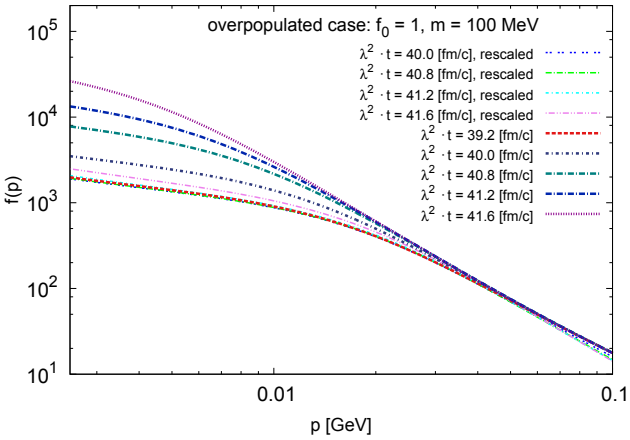

FIG. 12. Rescaled self-similar evolution of the one-particle distribution function in the in infrared region of the classical dynamics with $f\,(p) \gg 1$.

respect to the momentum p, by defining them as

$$\left(\frac{\mathrm{d}n}{\mathrm{d}p}\right)_{\mathrm{part}} := \frac{p^2 f_{\mathrm{part}}\,(t,p)}{2\pi^2 n_{\mathrm{tot}}}\,, \qquad \left(\frac{\mathrm{d}\epsilon}{\mathrm{d}p}\right)_{\mathrm{part}} := \frac{E p^2 f_{\mathrm{part}}\,(t,p)}{2\pi^2 \epsilon_{\mathrm{tot}}}\,. \tag{18}$$

In our approach with a finite particle mass the infrared region is of non-relativistic character, so according to (B14) the particle cascade should scale like a power law $1/p^{\alpha_4}$ with the exponent $\alpha_4 = 7/3$. Indeed, this is exactly the case as can be deduced from Figs. 9 and 10, supporting the picture of a stationary turbulence scaling in the infrared as reported in [19, 24]. Thereby our scaling exponent is equivalent to $\alpha = 7/6$, since the distribution function with respect to the momentum p scales like $1/p^{\alpha_4} \sim 1/E^{\alpha}$ for the classical dispersion relation.

In addition to the discussed non-relativistic and inverse particle cascade, we also observe an energy flow to the ultraviolet region with a different scaling behavior. For momenta $p \gg m = 100$ MeV the relativistic dispersion relation scales almost linearly with increasing momentum, and according to (B15) one should expect $\alpha_4 = 5/3$ to be the particular exponent of a direct energy cascade. Obviously, at intermediate times there is an excess of the energy density over the equilibrium value in the momentum range [0.1, 1] as seen in Fig. 11, which explains the origin of the energy cascade towards the ultraviolet. The stored energy in the infrared is negligibly small and is caused by a finite value of the particle mass. Effectively, there is no energy transport to the infrared and almost no particle transport to the ultraviolet as expected[6]. For $\lambda^2 t = 44$ fm/c the particle transport has already collapsed and the scaling is very close to the equilibrium one, since $\alpha_4 = 7/3$ is not a root of the full collision integral as given in (8), including the interaction between particles and the condensate. The direct energy cascade still exists as seen from Fig. 10, even though the condition (B6) is only partially fulfilled for $f_0 = 1$ as the initial distribution function. Accordingly, for larger momentum scales $p > 1$ GeV with $f\,(p) < 1$ quantum effects become important and dominate over the turbulent scaling behavior, leading to a significantly different evolution of the one-particle distribution function.

Based on our numerical results the system undergoes a self-similar evolution in the infrared for the inverse particle cascade and in the ultraviolet for the direct energy cascade, thereby both exponents can be explained by means of a stationary turbulent scaling. Nevertheless, at this point we also refer to [25, 26], where the authors study the universal self-similar dynamics by using classical-statistical lattice simulations and vertex-resummed kinetic theory, emphasizing that both are more reliable in the infrared sector of a strong turbulent scaling, arising for $f\,(p) \geq 1/\lambda \gg 1$ in contrast to a weak wave-turbulence, which exists in the region of $1/\lambda \gg f\,(p) \gg 1$.

Since in our case the infrared region scales analogously to the non-relativistic case and a time point τ_0 exists at which the condition (B6) is surely fulfilled, we can apply the same ansatz for the parametrization of the momentum distribution function as in [24]. Following their approach, we separate $f(\tau, p)$ in an amplitude function $A\,(\tau)$ with an exponent $-\beta$ and the one-particle distribution function at τ_0 with a rescaled momentum $q := p/A\,(\tau)$:

$$f\,(\tau, p) = A^{-\beta}\,(\tau)\, f\,(\tau_0, q)\,, \tag{19}$$

where τ is given by $\tau = t - \tau_0$. The amplitude function $A\,(\tau)$ describes the scaling behavior of the occupation number with respect to time. Inserting this ansatz in the

[6] In contrast a significant energy transport to the ultraviolet and turbulent particle transport to the infrared can be observed

isotropic Boltzmann equation (A10) without condensate, we derive in our case the following form

$$A(\tau) = \left(\frac{\tau_c - \tau}{\tau_c}\right)^{\frac{1}{2(\alpha_4-2)}} \tag{20}$$

by requiring $A(0) = 1$. Here, $\lambda^2(\tau_c + \tau_0) \approx 43.2$ fm/c defines the time point at which the distribution function for the zero mode grows to infinity $f(t, p = 0) \to \infty$. This value can be extracted numerically by setting $n_c = 0$ in (A11) and so forbidding the condensation process for all times. Furthermore, it turns out that $\beta \equiv \alpha_4$. In Fig. 12 we plotted the one-particle distribution function at five different times, starting with $\lambda^2 t = 39.2$ fm/c, which determines τ_0. In fact, the rescaled distribution functions lie almost on top of each other as expected from a self-similar evolution; only for the largest time $\lambda^2 t = 41.6$ fm/c we observe a deviation due to the condensation process which is not forbidden and starts already earlier, modifying[7] the turbulent scaling as the system approaches τ_c.

IV. SUMMARY

We have presented a numerical approach for treating the kinetics of Bose-Einstein condensation by decomposing the one-particle phase space distribution function into two parts. Thereby the zero-momentum part is given by a product of the condensate density and a δ-function in momentum space. The non-zero momentum part contains the distribution of excited modes. Inserting such an ansatz in the full Boltzmann equation and discretizing the external momentum leads to a coupled set of integro-differential equations for discrete modes. We have solved this set of equations by using a quadrature scheme for the numerical evaluation of the collision integrals and an adaptive Runge-Kutta scheme for the time propagation of the differential equations. We compared our results in the critical case to the partonic transport code BAMPS, which applies a test-particle Monte-Carlo ansatz to solve the Boltzmann equation. The time evolution of both simulations is in good agreement with a much better performance for our code in the kinetic regime of a relativistic Bose-Einstein condensate.

In the last Section we have initialized a strongly overpopulated system of massive scalar bosons and have shown that our kinetic approach leads to an accurate description of the equilibration process, evolving the system exactly to the expected values for the temperature, chemical potential and the condensate value. In this overpopulated case the time evolution shows a typical particle cascade to the infrared momentum region, developing in a self-similar way with a non-relativistic scaling exponent in the inertial region of turbulent dynamics. Here, the occupation numbers of soft modes overshoot the equilibrium values by several orders of magnitude, followed by a relaxation to the equilibrium curve because of the condensation process. In contrast the energy flow to the ultraviolet region evolves with a relativistic exponent, confirming a weak wave turbulence scaling.

In a future work we will include other types of matrix elements which can be directly applied to the formation of a condensate like state of gluons in the initial state of a heavy ion collision. Particularly, the impact of the particle changing process $2 \leftrightarrow 3$ could avoid the formation of a condensate and has to be studied in detail. Therefore we will also include a Bjorken expansion along the rapidity axis with an anisotropic distribution function in $(2+1)$ dimensions. Furthermore, the presented numerical approach is part of a code based on an on-shell approximation of self-consistent quantum kinetic equations from the 2PI effective action of the linear σ model with constituent quarks and will be used for the study of dynamical fluctuations during the chiral phase transition.

[7] The collision integral for the interaction with the condensate begins to grow rapidly.

ACKNOWLEDGMENTS

A. M. acknowledges support from the Helmholtz Research School for Quark Matter Studies (H-QM) and HIC for FAIR. HvH. has been supported by the Deutsche Forschungsgemeinschaft (DFG) under grant number GR 1536/8-1. K. Z. was supported by the Helmholtz International Center for FAIR within the framework of the LOEWE program launched by the State of Hesse. Numerical computations have been performed at the Center for Scientific Computing (CSC).

Appendix A: Isotropic Boltzmann equation

In the case of a ϕ^4-interaction with $\frac{1}{\nu}|\mathcal{M}_{12\to34}|^2 = 18\lambda^2$ one can integrate out the angular dependence in (4) by simply using the Fourier transform of the momentum conserving δ-function

$$\begin{aligned}\delta^{(3)}(\vec{p}) &= \int_{\mathbb{R}^3} \frac{\mathrm{d}^3 q}{(2\pi)^3} \exp\left(-\mathrm{i}\vec{p}\cdot\vec{q}\right) \\ &= \int_0^\infty \mathrm{d}q\, q^2 \int_0^{2\pi} \mathrm{d}\varphi \int_0^\pi \mathrm{d}\vartheta_q \sin\vartheta_q \\ &\qquad \exp\left[-\mathrm{i}pq\cos\vartheta_q\right] \\ &= \int_0^\infty \mathrm{d}q\, q^2 \left[\frac{4\pi}{pq}\sin(pq)\right],\end{aligned} \tag{A1}$$

leading to the isotropic form of the Boltzmann equation,

$$\begin{aligned}\partial_t f_1 = \frac{9\lambda^2}{8\pi^4}\int_0^\infty \mathrm{d}p_2\,\mathrm{d}p_3\,\mathrm{d}p_4\,\mathrm{d}q \frac{1}{E_1E_2E_3E_4} \\ \times \delta\left(E_1+E_2-E_3-E_4\right)\frac{p_2p_3p_4}{p_1q^2} \\ \times \sin\left(p_1q\right)\sin\left(p_2q\right)\sin\left(p_3q\right)\sin\left(p_4q\right) \\ \times \left[\left(1+f_1\right)\left(1+f_2\right)f_3f_4 \right. \\ \left. - f_1f_2\left(1+f_3\right)\left(1+f_4\right)\right].\end{aligned} \tag{A2}$$

Defining an auxiliary function which depends on the involved momenta

$$\mathcal{F}^{p_1}_{1,2\leftrightarrow3,4} = \int_0^\infty \mathrm{d}q \frac{\sin\left(p_1q\right)\sin\left(p_2q\right)\sin\left(p_3q\right)\sin\left(p_4q\right)}{p_1q^2}, \tag{A3}$$

and integrating out the q-dependence leads to

$$\begin{aligned}\mathcal{F}^{p_1=0}_{1,2\leftrightarrow3,4} = \frac{\pi}{8}\Big[&\operatorname{sign}\left(p_2+p_3-p_4\right) \\ &- \operatorname{sign}\left(p_2-p_3-p_4\right) \\ &+ \operatorname{sign}\left(p_2-p_3+p_4\right) \\ &- \operatorname{sign}\left(p_2+p_3+p_4\right)\Big],\end{aligned} \tag{A4}$$

$$\begin{aligned}\mathcal{F}^{p_1>0}_{1,2\leftrightarrow3,4} = \frac{\pi}{16p_1}\Big[&\left|p_1-p_2-p_3-p_4\right| \\ &- \left|p_1+p_2-p_3-p_4\right| \\ &- \left|p_1-p_2+p_3-p_4\right| \\ &+ \left|p_1+p_2+p_3-p_4\right| \\ &- \left|p_1-p_2-p_3+p_4\right| \\ &+ \left|p_1+p_2-p_3+p_4\right| \\ &+ \left|p_1-p_2+p_3+p_4\right| \\ &- \left|p_1+p_2+p_3+p_4\right|\Big],\end{aligned} \tag{A5}$$

where the form of $\mathcal{F}^{p_1}_{1,2\leftrightarrow3,4}$ depends especially on the incoming momentum p_1. The remaining energy conserving δ-function is used to reduce the dimension of the integral by writing

$$\delta\left(E_1+E_2-E_3-E_4\right) = \frac{E_4}{p_4}\delta\left(p_4-\tilde{p}_4\right). \tag{A6}$$

Here $\tilde{p}_4$ is given via energy-momentum conservation with the relativistic dispersion relation

$$\tilde{p}_4 = \sqrt{\left(E_1+E_2-E_3\right)^2 - m_4^2}. \tag{A7}$$

Finally, one ends up with the following expression for the isotropic Boltzmann equation

$$\begin{aligned}\partial_t f_1 = \frac{9\lambda^2}{8\pi^4}\int_0^\infty \mathrm{d}p_2\int_0^\infty \mathrm{d}p_3 \frac{p_2p_3}{E_1E_2E_3}\theta\left(\tilde{p}_4^2\right)\mathcal{F}^{p_1}_{1,2\leftrightarrow3,4} \\ \times \left[\left(1+f_1\right)\left(1+f_2\right)f_3f_4 \right. \\ \left. - f_1f_2\left(1+f_3\right)\left(1+f_4\right)\right],\end{aligned} \tag{A8}$$

where the θ-function ensures that $\tilde{p}_4^2 \geq 0$.

In analogy to (A3) one can define the auxiliary functions

$$\begin{aligned}\mathcal{F}^{p_2=0}_{1,2\leftrightarrow3,4} &= \int_0^\infty \mathrm{d}q \frac{\sin\left(p_1q\right)\sin\left(p_3q\right)\sin\left(p_4q\right)}{p_1q}, \\ \mathcal{F}^{p_3=0}_{1,2\leftrightarrow3,4} &= \int_0^\infty \mathrm{d}q \frac{\sin\left(p_1q\right)\sin\left(p_2q\right)\sin\left(p_4q\right)}{p_1q}, \\ \mathcal{F}^{p_4=0}_{1,2\leftrightarrow3,4} &= \int_0^\infty \mathrm{d}q \frac{\sin\left(p_1q\right)\sin\left(p_2q\right)\sin\left(p_3q\right)}{p_1q}.\end{aligned} \tag{A9}$$

By means of (A8) and (A9) the evolution equation for the distribution function (8) as well as the condensate density (10) can be written in their final isotropic form

$$\begin{aligned}\partial_t f(t,p_1) = \frac{9\lambda^2}{8\pi^4}\int_0^\infty \mathrm{d}p_2\int_0^\infty \mathrm{d}p_3 \frac{p_2p_3}{E_1E_2E_3} \\ \times \theta\left(\tilde{p}_4^2\right)\mathcal{F}^{p_1>0}_{1,2\leftrightarrow3,4} \\ \times \left[\left(1+f_1\right)\left(1+f_2\right)f_3f_4 \right. \\ \left. - f_1f_2\left(1+f_3\right)\left(1+f_4\right)\right] \\ + \frac{9\lambda^2}{4\pi^2}\int_0^\infty \mathrm{d}p_3 \frac{p_3}{E_1E_2E_3}\theta\left(\tilde{p}_4^2\right)\mathcal{F}^{p_2=0}_{1,2\leftrightarrow3,4} \\ \times n_\mathrm{c}\left[f_3f_4 - f_1\left(1+f_3+f_4\right)\right] \\ + \frac{9\lambda^2}{4\pi^2}\int_0^\infty \mathrm{d}p_2 \frac{p_2}{E_1E_2E_3}\theta\left(\tilde{p}_4^2\right)\mathcal{F}^{p_3=0}_{1,2\leftrightarrow3,4} \\ \times n_\mathrm{c}\left[\left(1+f_1+f_2\right)f_4 - f_1f_2\right] \\ + \frac{9\lambda^2}{4\pi^2}\int_0^\infty \mathrm{d}p_2 \frac{p_2}{E_1E_2E_4}\theta\left(\tilde{p}_3^2\right)\mathcal{F}^{p_4=0}_{1,2\leftrightarrow3,4} \\ \times n_\mathrm{c}\left[\left(1+f_1+f_2\right)f_3 - f_1f_2\right],\end{aligned} \tag{A10}$$

$$\begin{aligned}\partial_t n_\mathrm{c}(t) = \frac{9\lambda^2}{8\pi^4}\int_0^\infty \mathrm{d}p_2\int_0^\infty \mathrm{d}p_3 \frac{p_2p_3}{E_1E_2E_3} \\ \times \theta\left(\tilde{p}_4^2\right)\mathcal{F}^{p_1=0}_{1,2\leftrightarrow3,4} \\ \times n_\mathrm{c}\left[f_3f_4 - f_2\left(1+f_3+f_4\right)\right].\end{aligned} \tag{A11}$$

Appendix B: Turbulent scaling

The derivations in this section are based on methods and ideas described in [27]. The relativistic integration measure of the Boltzmann equation (4) has the form

$$\begin{aligned}\mathrm{d}\Omega := &\frac{\left(2\pi\right)\delta^{(4)}\left(P_1+P_2-P_3-P_4\right)}{2\omega\left(\vec{p}_1\right)} \\ &\times \frac{\left|\mathcal{M}_{12\to34}\right|^2}{\nu}\prod_{i=2}^4 \frac{\mathrm{d}^3\vec{p}_i}{2\omega\left(\vec{p}_i\right)},\end{aligned} \tag{B1}$$

where $\omega\left(\vec{p}\right)$ is given by the energy-momentum dispersion relation. For an isotropic and homogeneous system this relation depends only on the modulus p of the momentum

vector $\vec{p}$ and scales like

$$\omega(p) = s^{-z}\omega(sp) \simeq \begin{cases} s^{-1}\omega(sp) & \text{for } p \gg m \text{ (relativistic)} \\ s^{-2}\omega(sp) & \text{for } p \ll m \text{ (non-relativistic)} \end{cases} \tag{B2}$$

with the dynamic exponent z, describing the scaling behavior of the energy $\omega(p)$ with respect to p. With the definition (B1) the collision integral of non-zero modes can be written as

$$\mathcal{C}_{2\mathrm{p}\leftrightarrow 2\mathrm{p}} \sim \int \mathrm{d}\Omega \left[(1+f_1)(1+f_2) f_3 f_4 - f_1 f_2 (1+f_3)(1+f_4) \right]. \tag{B3}$$

Focusing only on systems with a homogeneous scaling of the integration measure, one obtains

$$\mathrm{d}\Omega(sp_1, \dots, sp_4) = s^{\nu_4} \mathrm{d}\Omega(p_1, \dots, p_4) , \tag{B4}$$

where ν_4 denotes the scaling exponent of Ω. The index refers to the structure of the vertex with four interacting particles. From considering the integration measure in the relativistic (B1) and non-relativistic limit, where terms proportional to $1/\omega(p)$ become almost constant $\sim 1/m$, so that effectively only the energy-δ function contributes with the exponent -2 to the overall scaling behavior, ν_4 can be derived to be

$$\nu_4 = \begin{cases} 3d - (3+1) - 4z = 1 & \text{(relativistic)}, \\ 3d - (3+2) = 4 & \text{(non-relativistic)}, \end{cases} \tag{B5}$$

with $d \equiv 3$ denoting the number of dimensions. The term in brackets refers to an effective reduction of the dimensionality for the integration measure due to momentum and energy conservation.

Taking into account the large occupation number for the one-particle distribution function $f \gg 1$ in the inertial region of turbulent dynamics the Bose enhancement can be neglected and it follows

$$F := \left[(1+f_1)(1+f_2) f_3 f_4 - f_1 f_2 (1+f_3)(1+f_4) \right] \simeq \left[(f_1+f_2) f_3 f_4 - f_1 f_2 (f_3+f_4) \right], \tag{B6}$$

so in this regime only terms of the form f^3 contribute significantly to the integral, reducing the scaling complexity of the integral. Following the assumption of a power-law $f \sim 1/p^{\alpha_4}$ in the inertial region of the evolution, one obtains a homogeneous relation for the expression F with respect to the occupation number, respectively the momenta $p_1, \dots, p_4$.

$$F(sp_1, \dots sp_4) = s^{-3\alpha_4} F(p_1, \dots p_4) . \tag{B7}$$

This leads to a scaling exponent $\mu_4 := \nu_4 - 3\alpha_4$ for the full collision integral (B3),

$$\mathcal{C}_{2\mathrm{p}\leftrightarrow 2\mathrm{p}}[F](sp_1) = s^{\mu_4} \mathcal{C}_{2\mathrm{p}\leftrightarrow 2\mathrm{p}}[F](p_1) , \tag{B8}$$

where it is pointed out that $C_{2\mathrm{p}\leftrightarrow 2\mathrm{p}}$ is a functional with respect to F and depends explicitly on the external momentum p_1.

In the next step, one includes conservation laws, more precisely particle and energy densities by using the relations given in (14), but integrating only up to a finite value of the external momentum p_1. In an isotropic and homogeneous system the time evolution of the particle density in a momentum interval $[0, p]$ reads

$$\partial_t n_{\mathrm{part}}(t,p) := \int_0^p \frac{\mathrm{d}p_1 p_1^2}{2\pi^2} \partial_t f_{\mathrm{part}}(t, p_1) = \int_0^p \frac{\mathrm{d}p_1 p_1^2}{2\pi^2} \mathcal{C}_{2\mathrm{p}\leftrightarrow 2\mathrm{p}}[F](p_1) . \tag{B9}$$

Consequently, this expression is proportional to the isotropic particle flux in or out of a sphere with radius p and has to be constant as well as independent of the momentum-scale in the region of stationary turbulence. That means a rescaling of the argument in (B9) leads to

$$\partial_t n_{\mathrm{part}}(t,p) = \int_0^p \frac{\mathrm{d}p_1 p_1^2}{2\pi^2} s^{-\mu_4} \mathcal{C}_{2\mathrm{p}\leftrightarrow 2\mathrm{p}}[F](sp_1) . \tag{B10}$$

In analogy to the particle density one obtains the following relation for the energy density:

$$\partial_t \epsilon_{\mathrm{part}}(t,p) = \int_0^p \frac{\mathrm{d}p_1 p_1^2}{(2\pi)^3} s^{-z-\mu_4} \omega(sp_1)\, \mathcal{C}_{2\mathrm{p}\leftrightarrow 2\mathrm{p}}[F](sp_1) . \tag{B11}$$

Since the physics has to be scale invariant, one is free to choose $s = 1/p_1$, resulting in

$$\partial_t n_{\mathrm{part}}(t,p) \sim \frac{p^{d+\mu_4}}{d+\mu_4} C_{2\mathrm{p}\leftrightarrow 2\mathrm{p}}[F](1) \tag{B12}$$

for the particle as well as

$$\partial_t \epsilon_{\mathrm{part}}(t,p) \sim \frac{p^{d+z+\mu_4}}{d+z+\mu_4} \omega(1)\, C_{2\mathrm{p}\leftrightarrow 2\mathrm{p}}[F](1) . \tag{B13}$$

for the energy flux.

Due to the conservation of the particle density a scale invariant solution requires according to relation (B12) the following scaling behavior of the one-particle distribution function,

$$d + \mu_4 = d + \nu_4 - 3\alpha_4 \stackrel{!}{=} 0 \Rightarrow \alpha_4 = \begin{cases} 4/3 & \text{(relativistic)} \\ 7/3 & \text{(non-relativistic)}. \end{cases} \tag{B14}$$

Similarly, the exponent due to the conservation of the energy density reads

$$d + z + \mu_4 = d + z + \nu_4 - 3\alpha_4 \stackrel{!}{=} 0 \Rightarrow \alpha_4 = \begin{cases} 5/3 & \text{(relativistic)} \\ 8/3 & \text{(non-relativistic)}. \end{cases} \tag{B15}$$

From Eqs. (B12) and (B13) one immediately recognizes that the scaling conditions (B14), (B15) for a stationary turbulence imply roots of a first degree for the collision integral, otherwise the fluxes could not have a constant and finite value.

[1] C. C. Bradley, C. A. Sackett, J. J. Tollett, and R. G. Hulet, Phys. Rev. Lett. **75**, 1687 (1995).

[2] C. G. Böhmer and T. Harko, Journal of Cosmology and Astroparticle Physics **2007**, 025 (2007).

[3] D. P. Menezes, P. K. Panda, and C. Providencia, Phys. Rev. C **72**, 035802 (2005), arXiv:astro-ph/0506196 [astro-ph].

[4] M. G. Alford, A. Schmitt, K. Rajagopal, and T. Schäfer, Rev. Mod. Phys. **80**, 1455 (2008).

[5] S. O. Demokritov, V. E. Demidov, O. Dzyapko, G. A. Melkov, A. A. Serga, B. Hillebrands, and A. N. Slavin, Nature **443**, 430 (2006).

[6] H. van Hees, C. Wesp, A. Meistrenko, and C. Greiner, *Proceedings, 31st Max Born Symposium and HIC for FAIR Workshop : Three Days of critical behaviour in hot and dense QCD*, Acta Phys. Polon. Supp. **7**, 59 (2014), arXiv:1311.6825 [hep-ph].

[7] A. Meistrenko, C. Wesp, H. van Hees, and C. Greiner, *Proceedings, FAIR Next Generation Scientists (FAIRNESS 2013)*, J. Phys. Conf. Ser. **503**, 012003 (2014), arXiv:1311.7444 [hep-ph].

[8] C. Wesp, H. van Hees, A. Meistrenko, and C. Greiner, Phys. Rev. E **91**, 043302 (2015), arXiv:1411.7979 [hep-ph].

[9] C. Greiner, C. Wesp, H. van Hees, and A. Meistrenko, in *31th Winter Workshop on Nuclear Dynamics (WWND 2015) Keystone Resort, Colorado, USA, January 25-31, 2015* (2015) arXiv:1505.04738 [hep-ph].

[10] L. D. McLerran, *Lectures on quark matter. Proceedings, 40. International Universitaetswochen for theoretical physics, 40th Winter School, IUKT 40*, Lect. Notes Phys. **583**, 291 (2002), arXiv:hep-ph/0104285 [hep-ph].

[11] J.-P. Blaizot, F. Gelis, J.-F. Liao, L. McLerran, and R. Venugopalan, Nucl. Phys. A **873**, 68 (2012), arXiv:1107.5296 [hep-ph].

[12] J.-P. Blaizot, J. Liao, and L. McLerran, Nucl. Phys. A **920**, 58 (2013), arXiv:1305.2119 [hep-ph].

[13] J.-P. Blaizot, B. Wu, and L. Yan, Nucl. Phys. A **930**, 139 (2014), arXiv:1402.5049 [hep-ph].

[14] F. Scardina, D. Perricone, S. Plumari, M. Ruggieri, and V. Greco, Phys. Rev. C **90**, 054904 (2014), arXiv:1408.1313 [nucl-th].

[15] Z. Xu, K. Zhou, P. Zhuang, and C. Greiner, Phys. Rev. Lett. **114**, 182301 (2015), arXiv:1410.5616 [hep-ph].

[16] X.-G. Huang and J. Liao, Phys. Rev. D **91**, 116012 (2015), arXiv:1303.7214 [nucl-th].

[17] Z. Xu and C. Greiner, Phys. Rev. C **71**, 064901 (2005), arXiv:hep-ph/0406278 [hep-ph].

[18] Z. Xu and C. Greiner, Phys. Rev. C **76**, 024911 (2007), arXiv:hep-ph/0703233 [hep-ph].

[19] D. V. Semikoz and I. I. Tkachev, Phys. Rev. Lett. **74**, 3093 (1995).

[20] T. Epelbaum, F. Gelis, N. Tanji, and B. Wu, Phys. Rev. D **90**, 125032 (2014).

[21] G. P. Lepage, Journal of Computational Physics **27**, 192 (1978).

[22] J. R. Cash and A. H. Karp, ACM Trans. Math. Softw. **16**, 201 (1990).

[23] T. Epelbaum, F. Gelis, S. Jeon, G. Moore, and B. Wu, JHEP **09**, 117 (2015), arXiv:1506.05580 [hep-ph].

[24] D. V. Semikoz and I. I. Tkachev, Phys. Rev. D **55**, 489 (1997), arXiv:hep-ph/9507306 [hep-ph].

[25] J. Berges and D. Sexty, Phys. Rev. Lett. **108**, 161601 (2012).

[26] A. P. Orioli, K. Boguslavski, and J. Berges, Phys. Rev. D **92**, 025041 (2015), arXiv:1503.02498 [hep-ph].

[27] R. Micha and I. I. Tkachev, Phys. Rev. D **70**, 043538 (2004), arXiv:hep-ph/0403101 [hep-ph].